Absence of Proton Channels in COS-7 Cells Expressing Functional NADPH Oxidase Components

Deri Morgan,[1] Vladimir V. Cherny,[1] Marianne O. Price,[2] Mary C. Dinauer,[2] and Thomas E. DeCoursey[1]

[1]Department of Molecular Biophysics and Physiology, Rush Presbyterian St. Luke's Medical Center, Chicago, IL 60612
[2]Herman B. Wells Center for Pediatric Research, Department of Pediatrics (Hematology/Oncology) and Medical and Molecular Genetics, James Whitcomb Riley Hospital for Children, Indiana University Medical Center, Indianapolis, IN 46202

ABSTRACT Nicotinamide adenine dinucleotide phosphate (NADPH) oxidase is an enzyme of phagocytes that produces bactericidal superoxide anion (O_2^-) via an electrogenic process. Proton efflux compensates for the charge movement across the cell membrane. The proton channel responsible for the H^+ efflux was thought to be contained within the gp91^{phox} subunit of NADPH oxidase, but recent data do not support this idea (DeCoursey, T.E., V.V. Cherny, D. Morgan, B.Z. Katz, and M.C. Dinauer. 2001. *J. Biol. Chem.* 276:36063–36066). In this study, we investigated electrophysiological properties and superoxide production of COS-7 cells transfected with all NADPH oxidase components required for enzyme function (COS_{phox}). The 7D5 antibody, which detects an extracellular epitope of the gp91^{phox} protein, labeled 96–98% of COS_{phox} cells. NADPH oxidase was functional because COS_{phox} (but not COS_{WT}) cells stimulated by phorbol myristate acetate (PMA) or arachidonic acid (AA) produced superoxide anion. No proton currents were detected in either wild-type COS-7 cells (COS_{WT}) or COS_{phox} cells studied at pH_o 7.0 and pH_i 5.5 or 7.0. Anion currents that decayed at voltages positive to 40 mV were the only currents observed. PMA or AA did not elicit detectable H^+ current in COS_{WT} or COS_{phox} cells. Therefore, gp91^{phox} does not function as a proton channel in unstimulated cells or in activated cells with a demonstrably functional oxidase.

KEY WORDS: phagocytes • gp91^{phox} • H^+ channels • superoxide • respiratory burst

INTRODUCTION

Nicotinamide adenine dinucleotide phosphate (NADPH)* oxidase is an important antibacterial enzyme of granulocytes that produces superoxide anion (Babior, 1999). This multicomponent complex comprises several cytosolic subunits and the membrane-bound cytochrome b_{558}, which is composed of two subunits (gp91^{phox} and p22^{phox}) that coordinate FAD and two heme moieties (Yu et al., 1998). Upon stimulation, the cytosolic components, p67^{phox}, p47^{phox}, and Rac, a small GTP binding protein, translocate to the membrane and interact with cytochrome b_{558} (DeLeo and Quinn, 1996). The assembled complex catalyses the oxidation of NADPH and the transfer of electrons across the membrane to extracellular oxygen, which is an electrogenic process (Henderson et al., 1987). The enzyme can be activated by the phorbol ester PMA and by arachidonic acid (Babior, 1999). Voltage-gated proton currents are also greatly enhanced by these stimuli (DeCoursey et al., 2000, 2001a; Cherny et al., 2001). H^+ efflux is thought to compensate electrically for electron movement through NADPH oxidase (Henderson et al., 1987, 1988).

It has been proposed that a proton channel exists within the gp91^{phox} subunit of the NADPH oxidase. This conclusion was based originally on studies of CHO cells transfected with gp91^{phox} in which H^+ channel function was deduced from pH changes monitored by fluorescent pH dyes (Henderson et al., 1995, 1997; Henderson, 1998). Using only indirect measurements it is difficult to assess the existence and properties of H^+ channels and to rule out the involvement of other mechanisms that transport H^+ equivalents. Two recent studies provide direct voltage-clamp evidence of H^+ currents in CHO, HEK-293, and COS-7 cells heterologously transfected with gp91^{phox} (Henderson and Meech, 1999; Maturana et al., 2001). However, neither study is convincing. Transfection of gp91^{phox} into HEK-293 cells simply increased the endogenous H^+ currents fourfold (Maturana et al., 2001). The putative H^+ cur-

Address correspondence to Tom DeCoursey, Department of Molecular Biophysics and Physiology, Rush Presbyterian St. Luke's Medical Center, 1750 W Harrison, Chicago, IL 60612. Fax: (312) 942-8711; E-mail: tdecours@rush.edu

*Abbreviations used in this paper: AA, arachidonic acid; CGD, chronic granulomatous disease; DPI, diphenylene iodonium chloride; NADPH, nicotinamide adenine dinucleotide phosphate; pH_i, intracellular pH; pH_o, extracellular pH; PMA, phorbol 12-myristate 13-acetate; SITS, 4-acetamido-4-isothiocyanostilbene-2,2'-disulphonic acid; SOD, superoxide dismutase; V_{rev}, reversal potential; WT, wild-type.

Portions of this work were previously published in abstract form (Morgan, D., V.V. Cherny, M.C. Dinauer, M.O. Price, and T.E. DeCoursey. 2002. *Biophys. J.* 82:625a).

rents in COS-7 cells transiently transfected with gp91^{phox} and studied in whole-cell configuration (Maturana et al., 2001) appear to reverse >100 mV positive to the Nernst potential for H^+, and thus were not proton selective. The currents in CHO cells reported by Henderson and Meech (1999) differ profoundly from H^+ currents in all phagocytes studied to date: they are much less sensitive to inhibition by Zn^{2+}, Zn^{2+} fails to slow τ_{act}, no H^+ current was detectable at pH_i 7.5 even though the currents at pH_i 6.9 were larger than native voltage-gated proton currents reported in any cell, and activation was at least an order-of-magnitude more rapid.

Nanda et al. (1994) found normal voltage-gated proton currents in human monocytes from chronic granulomatous disease (CGD) patients who lacked cytochrome b_{558}, strong evidence that neither gp91^{phox} nor p22^{phox} is a proton channel in unstimulated phagocytes. We demonstrated recently that gp91^{phox} does not mediate voltage-gated proton currents in the myelocytic PLB-985 cell line (DeCoursey et al., 2001b). Upon induction by dimethylformamide, PLB-985 cells express functional NADPH oxidase and are capable of producing superoxide anions (Zhen et al., 1993). PLB-985 cells in which gp91^{phox} was knocked out by gene targeting had large voltage-gated proton currents that were normal in every respect. Furthermore, PMA stimulation increased the H^+ conductance to a similar extent in wild-type (WT) and knockout cells. Similar results were obtained in neutrophils from CGD patients lacking gp91^{phox} expression. Therefore, gp91^{phox} does not mediate H^+ currents in resting or activated cells. However, these results do not completely exclude the possibility that gp91^{phox} might function as a proton channel. Because of the endogenous H^+ currents in PLB-985 cells and CGD neutrophils, a small contribution by gp91^{phox} might have been missed. Furthermore, one might propose that some other molecule might be up-regulated to compensate for the loss of gp91^{phox}, as frequently occurs in genetic knockout studies (Yang et al., 2001). Therefore we performed the converse of the knockout experiment by introducing gp91^{phox} into COS-7 cells, which have no endogenous H^+ currents (Maturana et al., 2001). Although the goal of this study was to search for proton currents, there were large anion currents in most COS-7 cells and these are described briefly. We report here that neither WT COS-7 cells (COS_{WT}) nor COS-7 cells transfected with the four main NADPH oxidase components, including gp91^{phox} (COS_{phox}), have detectable voltage-gated proton currents, nor were any induced by PMA stimulation. We conclude that under conditions in which NADPH oxidase activity can be demonstrated, gp91^{phox} does not function as a proton channel.

MATERIALS AND METHODS

Cell Preparation and Maintenance

Green monkey kidney cells (COS_{WT}) were obtained from American Type Culture Collection (CRL-1651). COS-7 cells stably transfected with the four main subunits of NADPH oxidase: gp91^{phox}, p22^{phox}, p47^{phox}, and p67^{phox} (COS_{phox} cells) were developed by Price and colleagues (Price et al., 2002). First, COS-7 cells were stably transfected with p22^{phox} and gp91^{phox}. These cells were then further modified by stable transfection with p47^{phox}, and p67^{phox} to produce COS_{phox} cells. Cells were maintained in Dulbecco's MEM (Sigma-Aldrich) as described previously (Yu et al., 1997), with the exception that media for COS_{phox} cells also contained three antibiotics to ensure selection of transformed cells: 2 μg ml^{-1} puromycin (Sigma-Aldrich), 0.8 mg ml^{-1} G418 (Sigma-Aldrich), and 175 μg ml^{-1} hygromycin (Sigma-Aldrich). COS_{phox} cells were split when 70% confluent. COS-7 cells are adherent and were harvested by incubation with 0.25% trypsin in 1 mM EDTA (GIBCO-BRL) for 5 min at 37°C. For electrophysiologic recordings, cells were allowed to attach to small glass coverslips. The cells were kept in suspension for the cytochrome *c* assays.

Electrophysiology

Whole cell and permeabilized patch recordings were performed as described previously (Cherny and DeCoursey, 1999; DeCoursey et al., 2000) using micropipettes pulled from 7052 glass (Garner Glass). Although COS cells tend to flatten in culture, we selected rounded cells for recording, because voltage-clamp control is better and because the superoxide assays were done with nonadherent (and hence rounded) cells. Some cells were nearly spherical and others were irregular in shape; we did not attempt to record from flat cells. The cell diameter was ~15–25 μm, and the capacity in whole-cell measurements was 14.4 ± 4.5 pF (mean ± SD) in 20 sequentially studied COS_{phox} cells. Whole-cell solutions (pipette and bath solutions) contained 100 mM buffer, 1 mM EGTA, 70 mM tetramethylammonium (TMA^+) methanesulfonate ($MeSO_3^-$), and 2 mM $MgCl_2$ or 3 mM $CaCl_2$, with an osmolarity of ~300 mOsm. Buffers were Mes for pH 5.5 and BES (N,N-bis[2-Hydroxyethyl]-2-aminoethanesulfonic acid) for pH 7.0 solutions. In some experiments the Cl^- concentration was increased by replacing $TMAMeSO_3$ with TMACl or with Ringer's solution (in mM: 160 NaCl, 4.5 KCl, 2 $CaCl_2$, 1 $MgCl_2$, and 5 HEPES). Permeabilized patch recordings were performed in solutions containing 100 mM $TMAMeSO_3$, 25 mM $(NH_4)_2SO_4$, 2 mM $MgCl_2$, 5 mM BES, 1 mM EGTA titrated to pH 7.0 with TMAOH. The purpose of the 50 mM NH_4^+ in the bath and pipette solutions was to clamp pH_i near pH_o (pH 7.0) (Grinstein et al., 1994; DeCoursey et al., 2000). Pipette solutions also contained 0.5–1 mg ml^{-1} amphotericin B (Sigma-Aldrich). Pipettes were filled after dipping the tip in amphotericin free solution. Experiments were done at 21°C or at room temperature (21–24°C). Currents were amplified using either Axopatch 200B (Axon Instruments, Inc.) or List EPC-7 (List Electronic) amplifiers and filtered at 100 or 200 Hz. PClamp8 (Axon Instruments, Inc.) or lab-generated software and an Indec Laboratory acquisition and display system (Indec Corporation) were used for data acquisition and manipulation.

Superoxide Anion (O_2^-) Production

Cells were harvested by incubating the adherent cells in trypsin/EGTA at 5°C for 10 min. They were centrifuged for 5 min at 2,000 *g* and resuspended in Hanks' Balanced Salt Solution (HBSS) without phenol red at 5×10^6 cells ml^{-1}. The assays were

performed by incubating cells (2.5×10^5 cells well^{-1}) at 37°C in 250 μl HBSS containing 75 μM cytochrome *c*. Kinetic assays were performed on a Ceres UV900 plate reader (Biotek Instruments) and superoxide production was quantified using an extinction coefficient of 21.1 mM cm^{-1} for cytochrome *c*. The superoxide assays were performed on the same batches of cells and during the same time period that the electrophysiological studies were done.

7D5 Antibody Staining

Cells were harvested by brief trypsinization, pelleted (1,200 rpm for 6 min at 4°C), resuspended in PBS as a wash, and pelleted. Cells were resuspended in PBS containing 10% normal goat serum and incubated for 30 min on ice to block nonspecific binding sites. Cells were pelleted again then resuspended in PBS at 10^7 cells/ml. One aliquot of cells (100 μl) was incubated with 100 μl 7D5 supernatant for 30 min on ice while a second aliquot was incubated with 2 μl of isotype control CD-117 antibody. PBS containing 0.1% BSA (1 ml) was added as a wash and the cells were pelleted. Cells were resuspended in PBS and incubated for 30 min on ice with FITC conjugated goat-anti-mouse secondary antibody (1:100 dilution). PBS containing 0.1% BSA (1 ml) was added as a wash, and the cells were pelleted and then resuspended in 500 μl PBS for fluorescence-activated cell sorter analysis using a FACSCalibur machine (Becton Dickinson) equipped with CellQuest software. A total of 10,000 cells were counted for each condition. Cells with very low fluorescence (comprising ≤7% of the total, and falling below the lower limit of the graph) were considered dead and were gated out. Staining with 7D5 was compared with staining with isotype control. Also, levels of 7D5 staining were compared in COS_{phox} cells and COS_{WT} cells.

RESULTS

COS-7 Cells Have Cl^- Currents

COS_{WT} and COS_{phox} cells were studied in whole-cell configuration in solutions lacking most permeant ions at pH_i 5.5 and pH_o 7, conditions favorable for detecting proton currents. Many cells appeared to become "leaky" within a few seconds of breaking the membrane patch. This "leak" reflected the appearance of a large time-independent conductance at the holding potential (–60 mV) and at all potentials negative to 40 mV. The properties of this conductance were similar in COS_{WT} (Fig. 1, A–C) and COS_{phox} cells (Fig. 1, D–F).

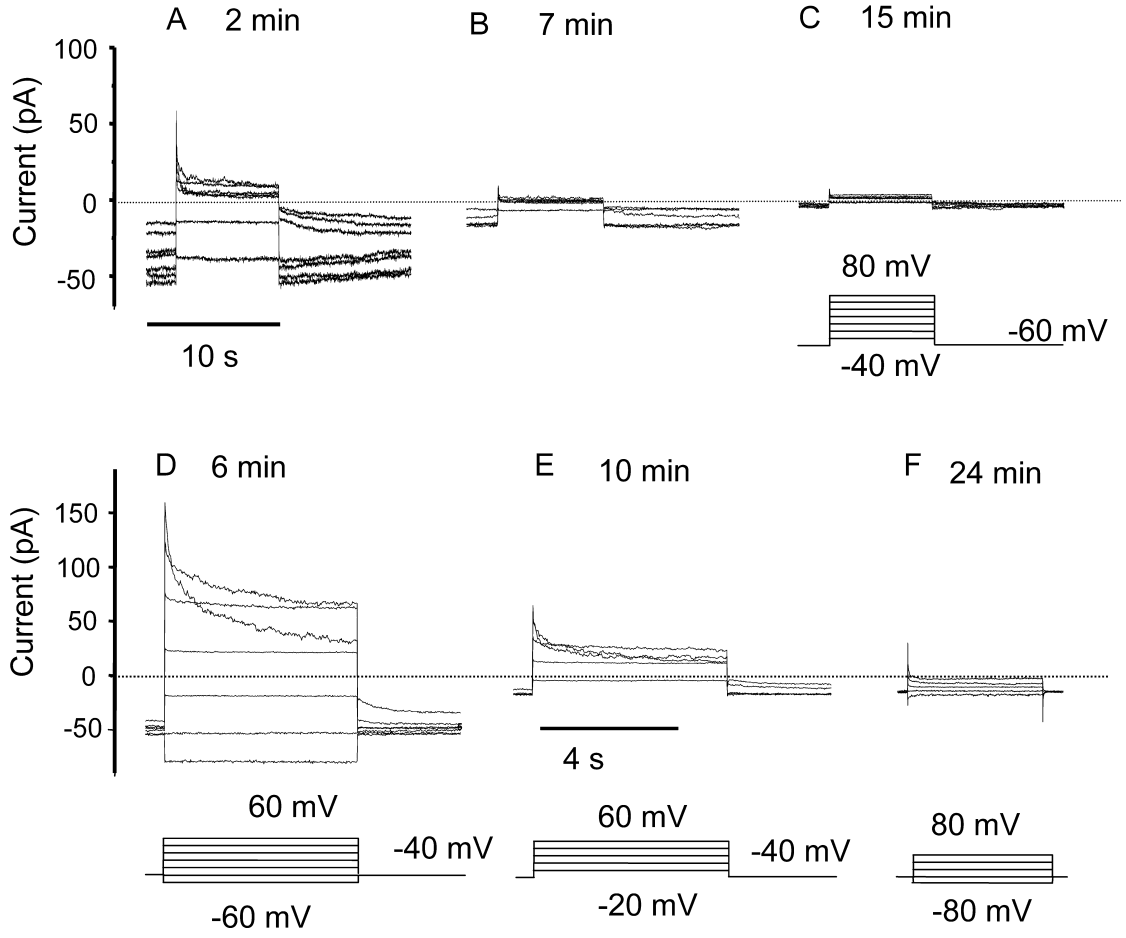

FIGURE 1. Rundown of whole-cell currents in COS_{WT} (A–C) and COS_{phox} (D–F) cells. Families of currents were recorded at various times after establishing whole cell configuration at pH_i 5.5 and pH_o 7.0 in $TMAMeSO_3$ solutions. Insets illustrate the voltage pulses, which were applied at an interval of 15 s. Results are representative of 6 COS_{WT} cells and 22 COS_{phox} cells. The current at the holding potential decreased progressively during most of the families of pulses illustrated.

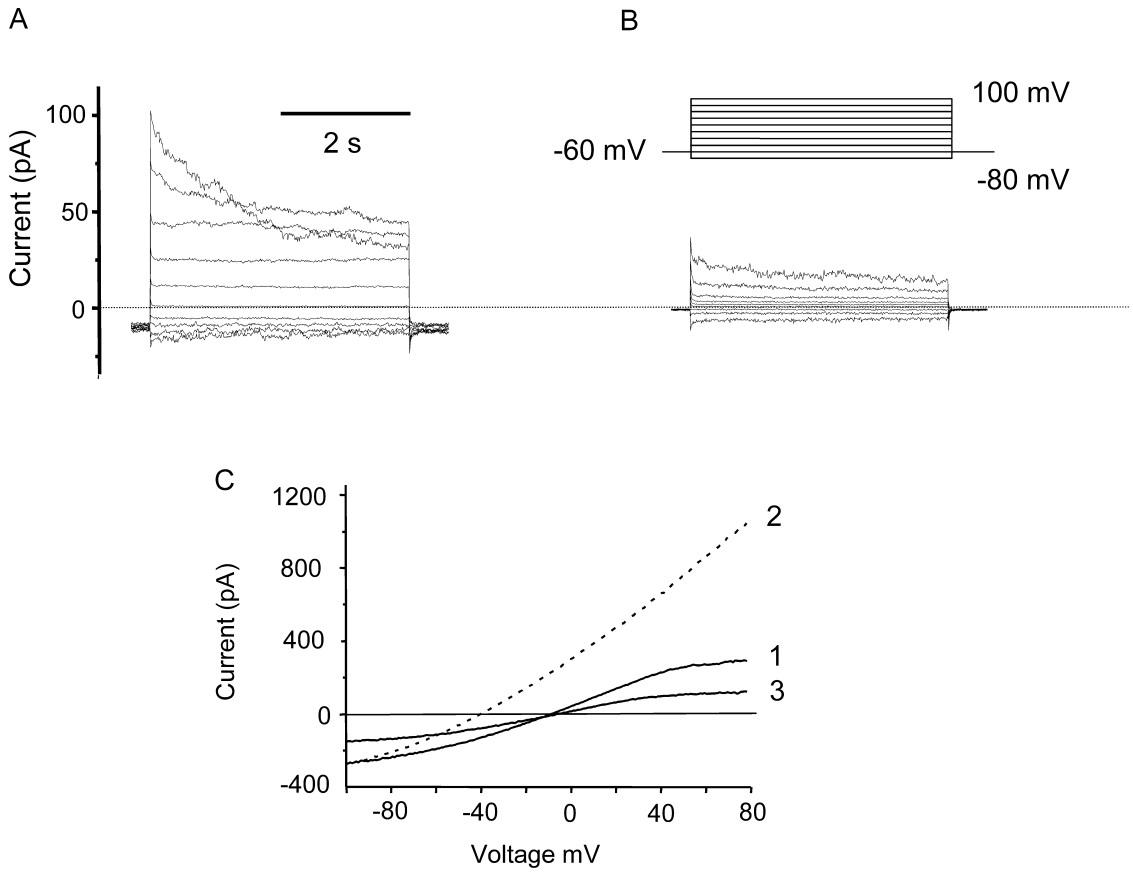

FIGURE 2. Characterization of the anion currents in COS_{phox} cells. Whole-cell current families are shown in a COS_{phox} cell in the absence (A) or in the presence (B) of the Cl^- channel blocker SITS (1 mM). Identical voltage pulse families were applied (inset), with an interval of 12 s at V_{hold} between pulses. (C) Currents recorded during voltage ramps from –100 to 80 mV in a COS_{phox} cell at 5 mM Cl^- (solid curves) or 166 mM Cl^- (dashed curve), labeled in the order recorded. Records 1, 2, and 3 were obtained ~9, 11, and 12 min after establishing whole-cell configuration, respectively.

During large depolarizing pulses the currents turned off with time. This decay reflected a genuine decrease in conductance because it was reversed upon repolarization; the inward currents were initially small and turned on with time. As evident in Fig. 1, the conductance decreased progressively after establishing whole-cell configuration in both COS_{WT} and COS_{phox} cells. The rundown produces a progressive decrease in holding current that is evident in some of the families. Eventually, only very small time-independent currents remained (Fig. 1, C and F).

The behavior of the currents in COS_{WT} and COS_{phox} cells, including the rundown phenomenon, was reminiscent of Cl^- currents in Chinese hamster ovary cells studied in similar solutions (Cherny et al., 1997). These currents resemble volume-regulated anion currents in several other epithelial cell types (McCann et al., 1989; Solc and Wine, 1991; Arreola et al., 1995). Fig. 2 shows the inhibition of whole-cell currents in a COS_{phox} cell by the traditional Cl^- channel blocker 4-acetamido-4'-isothiocyanostilbene-2,2'-disulfonic acid (SITS). The conductance decreased substantially at all potentials upon addition of SITS (Fig. 2 B), and was at least partially restored after wash out (unpublished data). To confirm the Cl^- selectivity of the conductance we ramped the voltage from −100 to 80 mV in solutions with different Cl^- concentrations (Fig. 2 C). Trace 1 shows ramp currents in symmetrical 5 mM Cl^- where the reversal potential (V_{rev}) was near 0 mV. Substituting the bath solution with 166 mM Cl^- increased the outward current at depolarizing voltages and shifted V_{rev} negative by 31 mV. Upon returning to the original solution, V_{rev} shifted back and the currents were reduced below the original levels, probably due to rundown (compare Fig. 1). The shift in V_{rev} is consistent with a relative permeability of ~0.5 for $MeSO_3^-$ compared with Cl^-, calculated by the Goldman-Hodgkin-Katz voltage equation after correction for liquid junction potentials. The outward current increased consistently in high [Cl^-]. The shift in V_{rev} was often less pronounced than in Fig. 2 C, but the shift in V_{rev} was larger when the anion conductance was large (i.e., shortly after establishing whole cell configuration). The predominant conductance in COS-7 cells was anion selective.

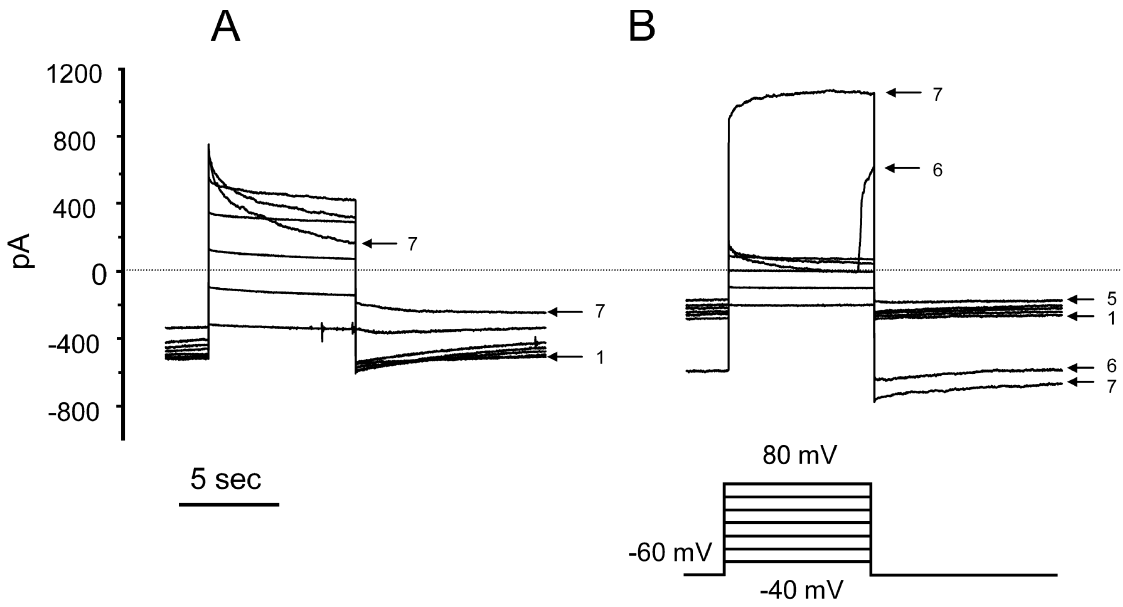

FIGURE 3. Sudden appearance of time-dependent outward current in a COS_{WT} cell, studied at pH_o 7.0 and pH_i 5.5. (A) A family of currents recorded starting 4 min after establishing whole-cell configuration displays behavior typical of the anion conductance. The pulses were applied in 20-mV increments up to 80 mV, at 30-s intervals. The entire family required ~3.5 min to complete. The first and last pulses are numbered, showing the progressive decrease in current at −60 mV. (B) A family recorded in the same cell shortly after the end of the previous family. The currents at all voltages including V_{hold} are scaled down, reflecting the rundown typically observed in these cells. In this cell during the pulse to 60 mV (pulse 6), there was a sudden catastrophic increase in leak current. The inward current upon repolarization was greatly increased. Interpolation of the current at the end of the pulse to 60 mV and that immediately after repolarization to −60 mV gives an estimated V_{rev} of 4 mV, suggesting a nonselective leak conductance. The subsequent pulse to 80 mV elicited an outward current that increased with time. Subsequent pulse families evoked time-independent leak current at all voltages, with a time-dependent increasing current at large positive voltages. Changing pH_o from 7.0 to 5.5 did not shift $V_{threshold}$ or elicit changes in gating kinetics normally seen in cells with voltage-gated H^+ currents. Addition of 100 μM $ZnCl_2$ did not inhibit the time-dependent outward currents. Although such currents bear a superficial resemblance to voltage-gated proton currents, they are artifacts.

COS-7 Cells Lack H^+ Currents

To identify putative voltage-gated proton currents, we waited for the anion conductance to subside and then looked for currents that increased with time during depolarizing pulses. In some cells time-dependent outward currents were seen, although typically this behavior was observed only after the input resistance had decreased markedly. An example is shown in Fig. 3. Normal behavior was observed early in this experiment on a COS_{WT} cell. The family of currents in Fig. 3 A was recorded starting 4 min after whole-cell configuration was established. Anion currents that are time independent except at large positive voltages were observed. The current at $V_{hold} = -60$ mV decreased progressively, in part because of progression of the rundown of anion currents during the 3.5 min required to record this family of long pulses. After the pulses to 60 and 80 mV that elicited decaying outward currents, the inward current upon repolarization was greatly reduced, reflecting the channel closing at positive voltages that is responsible for the current decay. The family of currents in Fig. 3 B was recorded in the same cell immediately after the previous family. By this time, the anion conductance had run down substantially and the currents at all voltages were scaled down, but otherwise exhibited similar time and voltage dependence. Near the end of the pulse to 60 mV (pulse 6), the current suddenly increased. The current at V_{hold} increased as well, and no recovery was observed before the next pulse, to 80 mV. During this last pulse (pulse 7), the current was much larger and there was a time-dependent increase in outward current during the pulse. Under normal circumstances, we would interpret the sudden increase in conductance to indicate damage to the cell membrane or loss of the seal. Such cells are usually considered to be "dead" and are discarded. However, because the time-dependent increasing outward currents superficially resemble voltage-gated proton currents, we continued recording. In cells with currents like these, changing pH_o did not change either V_{rev} or the threshold voltage for activating time-dependent outward current. These currents thus were not H^+ selective, nor did they display the pronounced pH_o sensitivity of gating of all voltage-gated proton channels (Eder and DeCoursey, 2001). Addition of 100 μM $ZnCl_2$ had no effect on the amplitude or kinetics of these currents. In summary, there was no credible evidence of voltage-

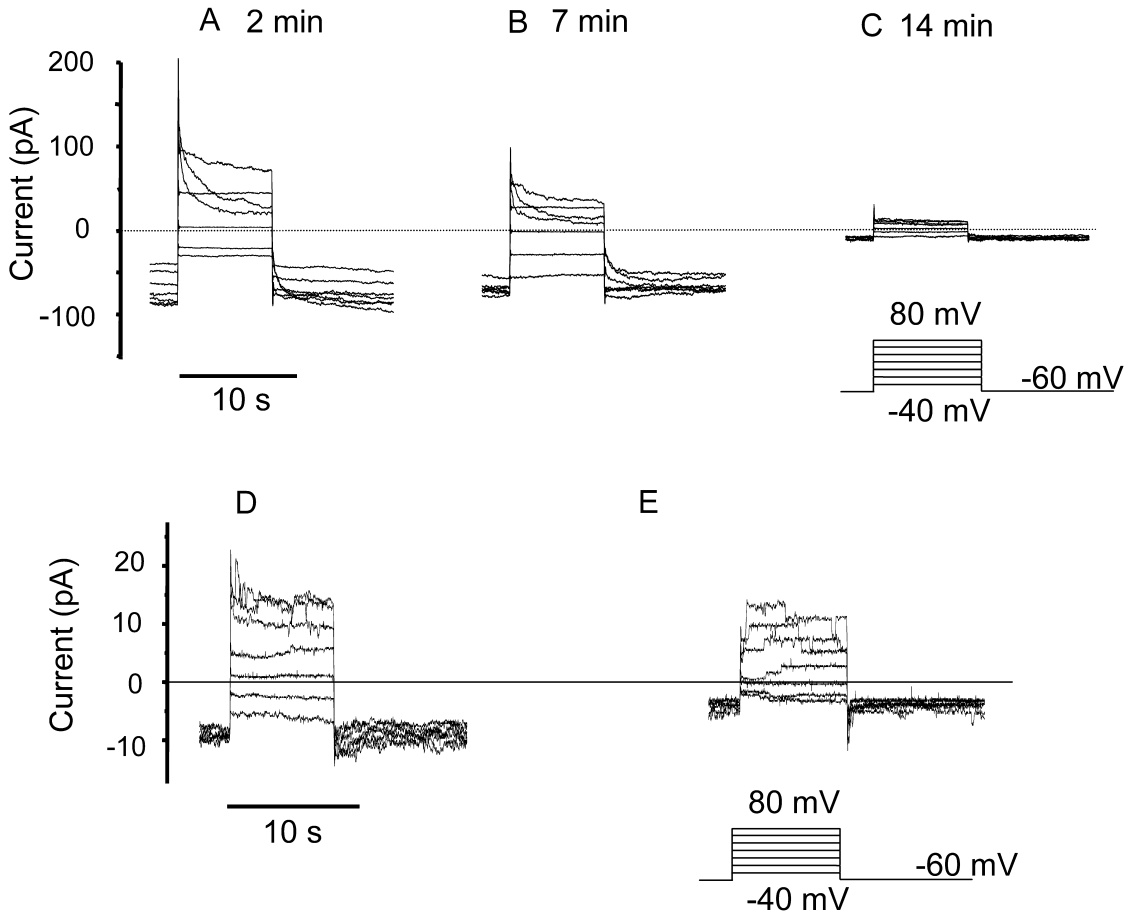

FIGURE 4. Lack of effect of PMA on membrane currents COS_{phox} cells in permeabilized patch configuration. (A–C) Families of voltage-clamp currents in a COS_{phox} cell in permeabilized patch configuration at the indicated times after beginning recording. The bath solution contained $TMAMeSO_3$ at pH 7.0, and both pipette and bath contained 50 mM NH_4^+ to clamp pH_i near pH_o. Currents at high gain in a COS_{phox} cell before (D) and 10 min after (E) addition of 60 nM PMA. No voltage-gated conductance was activated by PMA or AA in 45 cells studied in permeabilized patch configuration.

gated proton currents in any COS_{WT} or COS_{phox} cell studied.

To investigate whether stimuli that activate NADPH oxidase might induce or enhance proton currents, as has been observed in human neutrophils and eosinophils (DeCoursey et al., 2000, 2001a; Cherny et al., 2001) we used the permeabilized patch configuration, which preserves NADPH oxidase function (DeCoursey et al., 2000). Many unstimulated COS_{phox} cells in permeabilized patch configuration exhibited Cl^- currents that disappeared with time (Fig. 4, A–C), similar to the currents in whole-cell studies. Increasing $[Cl^-]_o$ increased the outward current and tended to shift V_{rev} to more negative voltages (unpublished data). No time-dependent currents were seen in COS_{phox} cells after the Cl^- currents ran down. In about one-third of COS_{phox} cells the anion conductance was small or absent throughout the experiment, and the currents were similar to those in Fig. 4 C.

Fig. 4, D and E, respectively, show families of currents at high gain before and 10 min after the addition of 60 nM PMA. No time-dependent currents appeared at any voltage after the addition of PMA in this cell. In Fig. 4, D and E, discrete current steps consistent with a single channel conductance of ~30 pS can be seen at some voltages. These currents are most likely conducted through anion channels similar to volume-sensitive anion channels reported previously (Solc and Wine, 1991). Single voltage-gated proton channel currents are too small to record directly (Byerly and Suen, 1989; DeCoursey and Cherny, 1993). Furthermore, 100 μM Zn^{2+} did not inhibit any component of the currents in PMA-treated COS_{phox} cells. Thus, both unstimulated (31 cells studied in whole-cell or permeabilized-patch configuration) and PMA- or AA-stimulated COS_{phox} cells ($n = 45$) lack detectable proton currents.

COS_{phox} Cells Express $gp91^{phox}$ and Produce Superoxide Anion (O_2^-)

To assess the efficiency of $gp91^{phox}$ expression in COS_{phox} cells, we used the 7D5 antibody, which is directed

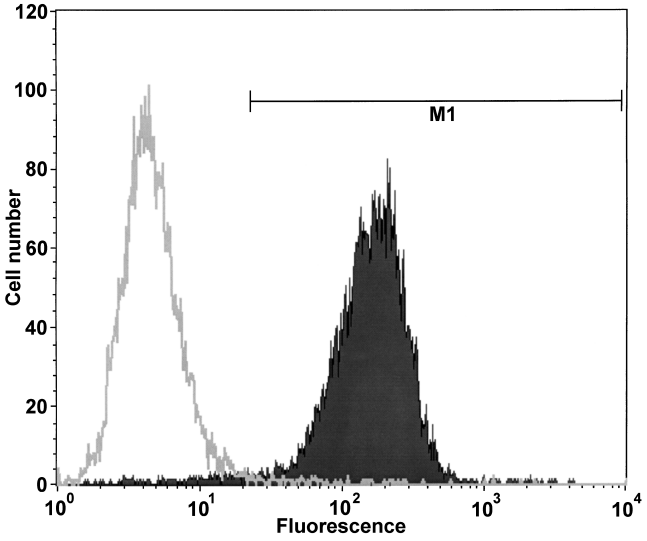

FIGURE 5. 7D5 antibody staining of COS_{phox} cells compared with COS_{WT} cells. Cells harvested by brief trypsinization were incubated with 7D5 monoclonal antibody, which recognizes an extracellular epitope of $gp91^{phox}$. Following incubation with a FITC-conjugated goat anti–mouse secondary antibody, cells were analyzed by flow cytometry. The marker M1 was set to exclude 99% of the COS_{WT} cells (open histogram), and indicates the range defined as positively stained. By this criterion, 98.3% of the COS_{phox} cells (solid histogram) were positively stained for $gp91^{phox}$ expression.

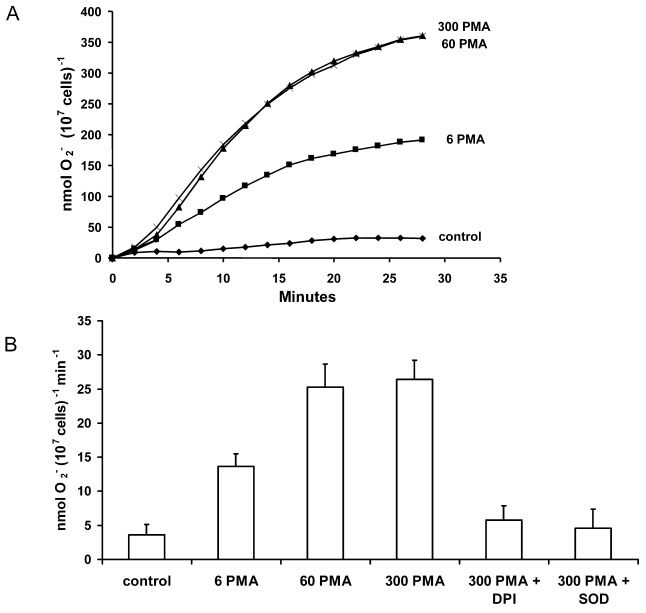

FIGURE 6. Superoxide production by COS_{phox} cells. (A) The average time course of PMA-stimulated superoxide anion production detected as the reduction of cytochrome *c* is plotted. Cells (10^6 cells/ml) were incubated at 37°C in HBSS before the addition of PMA (concentrations of PMA are in nM). Control cells were not stimulated. Data are mean values from four experiments with the error bars removed for clarity. (B) The average maximum rate of O_2^- production (± SE, $n = 4$) determined in each experiment in A. Data were collected in 2-min intervals and the rate is given per minute. DPI (6 μM) and 100 μg/ml SOD were added simultaneously with PMA to establish that the reduction of cytochrome *c* was due to NADPH oxidase and O_2^-, respectively.

against an extracellular epitope of the $gp91^{phox}$ molecule (Nakamura et al., 1988; Yu et al., 1998). Expression was tested in freshly thawed cells and passaged cells, in COS_{WT} and COS_{phox} cells, and with the CD-117 antibody as an isotype control. Fig. 5 illustrates histograms of the fluorescence intensity in COS_{WT} (open histogram) and COS_{phox} cells (solid histogram). 98% of the freshly thawed COS_{phox} cells (Fig. 5) and 96% of COS_{phox} cells maintained in culture for several weeks (unpublished data), as during the course of these experiments, stained positively for the 7D5 antibody. If cells with very low fluorescence (which presumably are dead cells) are included, then the 7D5-positive fraction is 95% of the freshly thawed COS_{phox} cells and 93% of COS_{phox} cells maintained in culture. Thus, the vast majority of COS_{phox} cells express $gp91^{phox}$ at the plasma membrane.

Superoxide anion (O_2^-) production by COS_{phox} cells was assessed by their ability to reduce ferricytochrome *c*. Fig. 6 A shows the average time courses of cumulative O_2^- release by four batches of COS_{phox} cells challenged with different concentrations of PMA. O_2^- production above control levels was seen at 6 nM PMA. PMA at 60 and 300 nM, respectively, produced similar levels of O_2^-. The O_2^- release time course was characterized by a delay of several minutes after the addition of PMA, followed by a rapid increase between 5 and 20 min, after which the rate of O_2^- production diminished. Fig. 6 B summarizes the average maximal rate of O_2^- production in these experiments. The highest maximal rate, observed at 300 nM PMA, was 26 ± 6 nmol min^{-1} $(10^7$ cells$)^{-1}$. The response was almost completely inhibited by 100 μg/ml superoxide dismutase (SOD), showing that ferricytochrome *c* reduction was due to the release of O_2^- and not peroxides or other oxidizing agents. Diphenylene iodonium (DPI) at 6 μM also inhibited O_2^- production, implicating a flavoenzyme (O'Donnell et al., 1994), most likely NADPH oxidase (Cross and Jones, 1986). As reported previously (Price et al., 2002), COS_{WT} cells studied under identical conditions did not produce detectable O_2^- (unpublished data).

Arachidonic acid (AA) can stimulate COS_{phox} cells to produce O_2^- at a higher rate than that stimulated by PMA (Price et al., 2002). We examined the time course of AA-stimulated O_2^- production in six assays (unpublished data). The onset of O_2^- production stimulated by 10–100 μM AA was faster than when PMA was used. However, the AA-stimulated respiratory burst was more transient, with little additional O_2^- released after 10–15 min, whereas PMA-stimulated O_2^- release continued over 30 min.

Because NADPH oxidase is electrogenic (Henderson et al., 1987), its activity can be detected electrically as a small inward current under favorable conditions

(Schrenzel et al., 1998; DeCoursey et al., 2000). Electron currents were difficult to detect in COS_{phox} cells, probably because the activity of NADPH oxidase is lower than in human neutrophils (Price et al., 2002) and the baseline currents were larger and less stable. These measurements were made at 0 to −20 mV to minimize the leak (anion) current amplitude. No convincing electron currents were seen with PMA as a stimulus. Because the maximal rate of O_2^- production in COS_{phox} cells is larger with AA than PMA as a stimulus (Price et al., 2002) and the onset is more rapid (present study), we also used AA as an agonist. Addition of 5–10 μM AA led to an increase in inward current of 1–2 pA in about half the cells tested, but only a fraction of this current was inhibited by 6–12 μM DPI. Because AA can induce nonspecific membrane leak (Meves, 1994; Cherny et al., 2001), we consider only inward current inhibitable by DPI in the presence of AA to indicate electron current. The mean DPI-inhibited inward current in COS_{phox} cells was −0.26 ± 0.10 pA (mean ± SE, $n = 21$). Although it is possible that these DPI-sensitive currents reflect genuine electron current, we conclude that the electron currents in COS_{phox} cells are too small to detect reliably.

DISCUSSION

Although the goal of this study was to search for voltage-gated proton currents in cells expressing $gp91^{phox}$, the only conductance found in COS_{phox} cells was anion selective. Cl^--selective currents similar to volume-sensitive Cl^- currents in many other epithelial cells (McCann et al., 1989; Solc and Wine 1991; Arreola et al., 1995; Cherny et al., 1997) were present shortly after establishing whole-cell configuration in most COS_{WT} and COS_{phox} cells. In an earlier study of CHO cells, small voltage-gated proton currents were revealed after the anion conductance ran down (Cherny et al., 1997), but in COS_{WT} and COS_{phox} cells no proton currents were ever observed. These results are consistent with the observation of Maturana et al. (2001) that COS_{WT} cells lack endogenous proton channels.

We saw no H^+ currents in COS-7 cells stably transfected with all four major components of the NADPH oxidase, including $gp91^{phox}$ (COS_{phox} cells). In some COS_{phox} and COS_{WT} cells we saw outward currents that increased during large depolarizing pulses. These currents, seen mainly in "leaky" cells, were not inhibited by 100 μM Zn^{2+}, a potent, classical inhibitor of voltage-gated proton channels (Cherny and DeCoursey, 1999), and neither V_{rev} nor the threshold potential was sensitive to pH_o, contrary to the properties of voltage-gated proton channels in all cells studied to date (Eder and DeCoursey, 2001). Thus, no credible evidence of voltage-gated proton currents was seen in any COS_{WT} or COS_{phox} cell. The maximum proton current in most phagocytes is ∼100 times greater than that required to fully compensate for the electron flux through NADPH oxidase (Eder and DeCoursey, 2001). If a comparable relationship existed in COS_{phox} cells, one would predict ∼50 pA of proton current. Even a few picoamperes of H^+ current would have been evident in COS_{phox} cells after rundown of the anion conductance.

In previous studies, evidence of proton flux was reported when $gp91^{phox}$ was expressed without any other NADPH oxidase components in CHO, HEK-293, and COS-7 cells (Henderson et al., 1995, 1997; Henderson 1998; Henderson and Meech, 1999; Maturana et al., 2001). However, the putative proton currents reported in patch-clamp studies of $gp91^{phox}$ expressed in the CHO and COS-7 heterologous expression systems (Henderson and Meech, 1999; Maturana et al., 2001) differ significantly from proton currents endogenous to phagocytes (see INTRODUCTION). It is conceivable that $gp91^{phox}$ expressed alone might function as an ion channel, and that this function is absent when it is coexpressed with $p22^{phox}$. If so, then $gp91^{phox}$ does not function as an ion channel under physiological conditions, because $gp91^{phox}$ is detectable in phagocyte membranes only together with $p22^{phox}$ in the flavocytochrome b_{558} heterodimer (Babior, 1999). The expression of $gp91^{phox}$ and $p22^{phox}$ are closely linked in neutrophils, where stable expression of either appears to be favored strongly by heterodimer formation, i.e., assembly to form flavocytochrome b_{558} (Roos et al., 1996; Yu et al., 1997; DeLeo et al., 2000).

The COS_{phox} cells in this study were transfected with all the components necessary for a fully functional oxidase. COS_{phox} cells released significant O_2^-, confirming that the oxidase was present in the plasma membrane and was functional. The maximum rate of PMA-stimulated O_2^- production at 37°C was 26 nmol $min^{-1}(10^7$ $cells)^{-1}$, comparable with the rate we reported previously in these cells (Price et al., 2002). The minimum efficiency of simultaneous expression of all four NADPH oxidase components was 69%, because this fraction was nitroblue tetrazolium (NBT)-positive in COS_{phox} cells (Price et al., 2002). NBT reduction indicates O_2^- production, and all four NADPH oxidase components are required for this function (Babior, 1999). Expression of $gp91^{phox}$ in COS_{phox} cells in the plasma membrane was confirmed by 7D5 antibody staining. The 7D5 antibody is directed against an extracellular epitope of $gp91^{phox}$ (Nakamura et al., 1988; Yu et al., 1998). That 96–98% of COS_{phox} cells were stained positively by the 7D5 antibody indicates that essentially all cells expressed $gp91^{phox}$ at the surface membrane.

Although COS_{phox} cells express a functional NADPH oxidase complex, attempts to detect electron currents that reflect the function of this enzyme were frustrated

by the presence of background (leak) currents, and by the tiny amplitude of these currents. The maximum rate of O_2^- production in COS_{phox} cells is less than one-fourth that in human neutrophils stimulated with PMA (Price et al., 2002). The electron current averages only −2.3 pA in human neutrophils (DeCoursey et al., 2000) and can be detected only because the input resistance in neutrophils is very high (usually >70 GΩ), and the background leak current was small (usually −0.6 pA or less) and stable. If electron currents in COS_{phox} were proportionately smaller they would be approximately −0.5 pA and consequently very difficult to detect; we did not detect electron currents in PMA-stimulated COS_{phox} cells. AA also stimulates O_2^- production in COS_{phox} cells (Price et al., 2002). Although AA induced small inward currents in some COS_{phox} cells, DPI reversed only a fraction of the current and thus the identification of these currents as genuine electron currents remains uncertain.

Bánfi et al. (1999) proposed that there were two types of H^+ channels in granulocytes; one in the resting cells and another that is active only when NADPH oxidase is active. Using the permeabilized patch configuration allowed us to investigate whether activating the oxidase might induce the appearance of H^+ currents in COS_{phox} cells. We have shown previously (DeCoursey et al., 2000, 2001a,b) that PMA stimulation of human neutrophils or eosinophils or PLB-985 cells in these conditions results in H^+ currents that closely resemble the NADPH oxidase–related H^+ currents described by Bánfi et al. (1999). AA also greatly enhances voltage-gated proton currents (Cherny et al., 2001). No time-dependent currents appeared after addition of PMA or AA to COS_{phox} cells. Evidently the enhancement of H^+ currents during the respiratory burst occurs only in cells that express voltage-gated proton channels in the resting state. This pattern is consistent with the idea that respiratory burst agonists modify the properties of preexisting H^+ channels (DeCoursey et al., 2000), rather than inducing the appearance of a new type of channel (Bánfi et al., 1999).

A curious point is that COS_{phox} cells devoid of proton channels are still capable of producing substantial O_2^-. The main function of voltage-gated proton channels in phagocytes is thought to be to provide a mechanism of charge compensation for the electron efflux through NADPH oxidase (Henderson et al., 1987; Eder and DeCoursey, 2001). Inhibiting H^+ currents reduces superoxide production in human neutrophils (Henderson et al., 1988) and eosinophils (Bankers-Fulbright et al., 2001) and in PLB cells (Lowenthal and Levy, 1999). Because anion currents were prominent in COS-7 cells, it is tempting to speculate that Cl^- influx may serve this function in lieu of H^+ efflux. In preliminary experiments SITS did not inhibit O_2^- release, but SITS did not completely inhibit Cl^- current (Fig. 2 A). The anion channel inhibitor 4,4-diisothiocyanostilbene-2,2'-disulfonic acid (DIDS) partially reduced O_2^- production in eosinophils (Schwingshackl et al., 2000). Alternatively, COS_{phox} cells may have some other mechanism of charge compensation.

The authors appreciate the able technical assistance of Tatiana Iastrebova.

This work was supported in part by the Heart, Lung, and Blood Institute of the National Institutes of Health (HL52671 and HL61437 to Dr. DeCoursey and HL45635 to Dr. Dinauer).

Submitted: 11 December 2001
Revised: 19 April 2002
Accepted: 22 April 2002

REFERENCES

Arreola, J., J.E. Melvin, and T. Begenisich. 1995. Volume-activated chloride channels in rat parotid acinar cells. *J. Physiol.* 484:677–687.

Babior, B.M. 1999. NADPH oxidase: an update. *Blood.* 93:1464–1476.

Bánfi, B., J. Schrenzel, O. Nüsse, D.P. Lew, E. Ligeti, K.-H. Krause, and N. Demaurex. 1999. A novel H^+ conductance in eosinophils: unique characteristics and absence in chronic granulomatous disease. *J. Exp. Med.* 190:183–194.

Bankers-Fulbright, J.L., H. Kita, G.J. Gleich, and S.M. O'Grady. 2001. Regulation of human eosinophil NADPH oxidase activity: a central role for PKCδ. *J. Cell. Physiol.* 189:306–315.

Byerly, L., and Y. Suen. 1989. Characterization of proton currents in neurones of the snail, *Lymnaea stagnalis*. *J. Physiol.* 413:75–89.

Cherny, V.V., and T.E. DeCoursey. 1999. pH-dependent inhibition of voltage-gated H^+ currents in rat alveolar epithelial cells by Zn^{2+} and other divalent cations. *J. Gen. Physiol.* 114:819–838.

Cherny, V.V., L.M. Henderson, and T.E. DeCoursey. 1997. Proton and chloride currents in Chinese hamster ovary cells. *Membr. Cell Biol.* 11:337–347.

Cherny, V.V., L.M. Henderson, W. Xu, L.L. Thomas, and T.E. DeCoursey. 2001. Activation of NADPH oxidase-related proton and electron currents in human eosinophils by arachidonic acid. *J. Physiol.* 535:783–794.

Cross, A.R., and O.T.G. Jones. 1986. The effect of the inhibitor diphenylene iodonium on the superoxide-generating system of neutrophils. Specific labelling of a component polypeptide of the oxidase. *Biochem. J.* 237:111–116.

DeCoursey, T.E., and V.V. Cherny. 1993. Potential, pH, and arachidonate gate hydrogen ion currents in human neutrophils. *Biophys. J.* 65:1590–1598.

DeCoursey, T.E., V.V. Cherny, W. Zhou, and L.L. Thomas. 2000. Simultaneous activation of NADPH oxidase-related proton and electron currents in human neutrophils. *Proc. Natl. Acad. Sci. USA.* 97:6885–6889.

DeCoursey, T.E., V.V. Cherny, A.G. DeCoursey, W. Xu, and L.L. Thomas. 2001a. Interactions between NADPH oxidase-related proton and electron currents in human eosinophils. *J. Physiol.* 535:767–781.

DeCoursey, T.E., V.V. Cherny, D. Morgan, B.Z. Katz, and M.C. Dinauer. 2001b. The $gp91^{phox}$ component of NADPH oxidase is not the voltage-gated proton channel in phagocytes, but it helps. *J. Biol. Chem.* 276:36063–36066.

DeLeo, F.R., and M.T. Quinn. 1996. Assembly of the phagocyte NADPH oxidase: molecular interaction of oxidase components. *J. Leukoc. Biol.* 60:677–691.

DeLeo, F.R., J.B. Burritt, L. Yu, A.J. Jesaitis, M.C. Dinauer, and W.M. Nauseef. 2000. Processing and maturation of flavocytochrome b_{558} include incorporation of heme as a prerequisite for heterodimer assembly. *J. Biol. Chem.* 275:13986–13993.

Eder, C., and T.E. DeCoursey. 2001. Voltage-gated proton channels in microglia. *Prog. Neurobiol.* 64:277–305.

Grinstein, S., R. Romanek, and O.D. Rotstein. 1994. Method for manipulation of cytosolic pH in cells clamped in the whole cell or perforated-patch configurations. *Am. J. Physiol.* 267:C1152-C1159.

Henderson, L.M. 1998. Role of histidines identified by mutagenesis in the NADPH oxidase-associated H^+ channel. *J. Biol. Chem.* 273: 33216–33223.

Henderson, L.M., G. Banting, and J.B. Chappell. 1995. The arachidonate-activatable, NADPH oxidase-associated H^+ channel: evidence that gp91-*phox* functions as an essential part of the channel. *J. Biol. Chem.* 270:5909–5916.

Henderson, L.M., J.B. Chappell, and O.T.G. Jones. 1987. The superoxide-generating NADPH oxidase of human neutrophils is electrogenic and associated with an H^+ channel. *Biochem. J.* 246: 325–329.

Henderson, L.M., J.B. Chappell, and O.T.G. Jones. 1988. Superoxide generation by the electrogenic NADPH oxidase of human neutrophils is limited by the movement of a compensating charge. *Biochem. J.* 255:285–290.

Henderson, L.M., and R.W. Meech. 1999. Evidence that the product of the human X-linked CGD gene, gp91-*phox*, is a voltage-gated H^+ pathway. *J. Gen. Physiol.* 114:771–785.

Henderson, L.M., S. Thomas, G. Banting, and J.B. Chappell. 1997. The arachidonate-activatable, NADPH oxidase-associated H^+ channel is contained within the multi-membrane-spanning N-terminal region of gp91-*phox*. *Biochem. J.* 325:701–705.

Lowenthal, A., and R. Levy. 1999. Essential requirement of cytosolic phospholipase A_2 for activation of the H^+ channel in phagocyte-like cells. *J. Biol. Chem.* 274:21603–21608.

Maturana, A., S. Arnaudeau, S. Ryser, B. Bánfi, J.P. Hossle, W. Schlegel, K.-H. Krause, and N. Demaurex. 2001. Heme histidine ligands within gp91^{phox} modulate proton conduction by the phagocyte NADPH oxidase. *J. Biol. Chem.* 276:30277–30284.

McCann, J.D., M. Li, and M.J. Welsh. 1989. Identification and regulation of whole-cell chloride currents in airway epithelium. *J. Gen. Physiol.* 94:1015–1036.

Meves, H. 1994. Modulation of ion channels by arachidonic acid. *Prog. Neurobiol.* 43:175–186.

Nakamura, M., S. Kobayashi, S. Sendo, T. Koga, and S. Kanegasaki. 1988. Deficiency of cytochrome b_{558} in chronic granulomatous disease demonstrated by monoclonal antibody 7D5. *Acta Paediatr. Hung.* 29:179–183.

Nanda, A., R. Romanek, J.T. Curnutte, and S. Grinstein. 1994. Assessment of the contribution of the cytochrome *b* moiety of the NADPH oxidase to the transmembrane H^+ conductance of leukocytes. *J. Biol. Chem.* 269:27280–27285.

O'Donnell, V.B., G.C.M. Smith, and O.T.G. Jones. 1994. Involvement of phenyl radicals in iodonium inhibition of flavoenzymes. *Mol. Pharmacol.* 46:778–785.

Price, M.O., L.C. McPhail, J.D. Lambeth, C.-H. Han, U.G. Knaus, and M.C. Dinauer. 2002. Creation of a genetic system for analysis of the phagocyte respiratory burst: high-level reconstitution of the NADPH oxidase in a nonhematopoietic system. *Blood.* 99: 2653–2661.

Roos, D., M. de Boer, F. Kuribayashi, C. Meischl, R.S. Weening, A.W. Segal, A. Åhlin, K. Nemet, J.P. Hossle, E. Bernatowska-Matuszkiewicz, and H. Middleton-Price. 1996. Mutations in the X-linked and autosomal recessive forms of chronic granulomatous disease. *Blood.* 87:1663–1681.

Schrenzel, J., L. Serrander, B. Bánfi, O. Nüsse, R. Fouyouzi, D.P. Lew, N. Demaurex, and K.-H. Krause. 1998. Electron currents generated by the human phagocyte NADPH oxidase. *Nature.* 392: 734–737.

Schwingshackl, A., R. Moqbel, and M. Duszyk. 2000. Involvement of ion channels in human eosinophil respiratory burst. *J. Allergy Clin. Immunol.* 106:272–279.

Solc, C.K., and J.J. Wine. 1991. Swelling-induced and depolarization-induced Cl^- channels in normal and cystic fibrosis epithelial cells. *Am. J. Physiol.* 261:C658-C674.

Yang, S., P. Madyastha, S. Bingel, W. Ries, and L. Key. 2001. A new superoxide-generating oxidase in murine osteoclasts. *J. Biol. Chem.* 276:5452–5458.

Yu, L., L. Zhen, and M.C. Dinauer. 1997. Biosynthesis of the phagocyte NADPH oxidase cytochrome b_{558}: role of heme incorporation and heterodimer formation in maturation and stability of gp91^{phox} and p22^{phox} subunits. *J. Biol. Chem.* 272:27288–27294.

Yu, L., M.T. Quinn, A.R. Cross, and M.C. Dinauer. 1998. Gp91^{phox} is the heme binding subunit of the superoxide-generating NADPH oxidase. *Proc. Natl. Acad. Sci. USA.* 95:7993–7998.

Zhen, L., A.A. King, Y. Xiao, S.J. Chanock, S.H. Orkin, and M.C. Dinauer. 1993. Gene targeting of X chromosome-linked chronic granulomatous disease locus in a human myeloid leukemia cell line and rescue by expression of recombinant gp91^{phox}. *Proc. Natl. Acad. Sci. USA.* 90:9832–9836.